Nonlinear Propagation of Spherical Calcium Waves in Rat Cardiac Myocytes

Manfred H. P. Wussling and Henning Salz
Julius Bernstein Institute of Physiology, Martin Luther University Halle-Wittenberg, D-06097 Halle, Germany

ABSTRACT Spontaneous calcium waves in enzymatically isolated rat cardiac myocytes were investigated by confocal laser scanning microscopy (CLSM) using the fluorescent Ca^{2+}-indicator fluo-3 AM. As recently shown, a spreading wave of enhanced cytosolic calcium appears, most probably during Ca^{2+} overload, and is initiated by an elementary event called a "calcium spark." When measured by conventional fluorescence microscopy the propagation velocity of spontaneous calcium waves determined at several points along the cardiac myocyte was previously found to be constant. More precise measurements with a CLSM showed a nonlinear propagation. The wave velocity was low, close to the focus, and increased with increasing time and propagation length, approaching a maximum of 113 μm/s. This result was surprising, inasmuch as for geometrical reasons a decrease of the propagation velocity might be expected if the confocal plane is not identical with that plane where the focus of the wave was localized. It is suggested that the propagation velocity is essentially dependent on the curvature of the spreading wave. From the linear relationship of velocity versus curvature, a critical radius of 2.7 $\pm$ 1.4 μm (mean $\pm$ SD) was worked out, below which an outward propagation of the wave will not take place. Once released from a sufficiently extended cluster of sarcoplasmic reticulum release channels, calcium diffuses and will activate its neighbors. While traveling away, the volume into which calcium diffuses becomes effectively smaller than at low radii. This effect is the consequence of the summation of elementary events (Ca^{2+} sparks) and leads to a steeper increase of the cytosolic calcium concentration after a certain diffusion path length. Thus the time taken to reach a critical threshold of $[Ca^{2+}]_i$ at the neighboring calcium release sites decreases with decreasing curvature and the wave will propagate faster.

INTRODUCTION

A number of animal cells with different physiological functions have been reported to exhibit calcium waves, e.g., fertilized oocytes and endothelial or smooth muscle cells (Rooney and Thomas, 1993). It is generally accepted that in cardiac myocytes the mechanism of propagation reflects the interaction between several intracellular events: calcium-induced calcium release (CICR), calcium diffusion, and calcium reuptake (Wier and Blatter, 1991; Williams et al., 1992; Williams, 1993). Myocardial cells that show spontaneously spreading calcium waves may be considered a "slow motion model" for the CICR mechanism.

New knowledge about the development and propagation of calcium waves has been acquired by using a combination of two techniques: confocal microscopy and fluorescent calcium indicators. The advantage of confocal compared with conventional light microscopy is that out-of-focus information can be minimized, thus obtaining a thickness of optical sections of less than 1 μm (Niggli and Lederer, 1990). Recently a "calcium spark" phenomenon has been reported to appear within small regions of rat cardiac myocytes lasting a few tens of milliseconds (Cheng et al., 1993). From calculations of the ionic flux associated with a calcium spark, it was concluded that this phenomenon is the optical manifestation of the opening and closing of one or two ryanodine receptors in the membranes of the sarcoplasmic reticulum (SR). The probability that a calcium "spark" (or "macrospark") triggers a calcium wave increases with the amount of calcium stored in the sarcoplasmic reticulum (Cheng et al., 1993).

As far as we know, the propagation velocity of the front of spontaneous spherical calcium waves observed within and along myocardial cells has been found to be constant, generally, with both conventional light and confocal laser scanning microscopy (Capogrossi and Lakatta, 1985; Golovina et al., 1986; Stern et al., 1988; Ter Keurs et al., 1988; Berlin et al., 1989; Ishide et al., 1990; Wier and Blatter, 1991; Rooney and Thomas, 1993; Tang and Othmer, 1994). The migration of calcium ions by diffusion is limited by numerous obstacles in the myofibrillar space (such as mitochondria, nuclei, sarcoplasmic reticulum, contractile and elastic proteins, and cytoskeleton) and masked by repeated Ca^{2+} release and Ca^{2+} reuptake as well as calcium buffers. Undoubtedly, the determination of the diffusion coefficient is problematical. Reported data vary in the range between 10^{-4} and 10^{-3} mm^2/s (Kushmerick and Podolsky, 1969; O'Neill et al., 1990; Allbritton et al., 1992). In a recently published model of calcium dynamics that was proposed to quantitatively simulate the traveling of calcium waves in cardiac myocytes (Tang and Othmer, 1994), the diffusion coefficient was set at $5 * 10^{-4}$ mm^2/s, resulting in a wave speed of 81 μm/s. Although the diffusion coefficients are assumed to be similar in cells with IP_3-sensitive endo-

Received for publication 23 May 1995 and in final form 7 November 1995.
Address reprint requests to Dr. Manfred H. P. Wussling, Julius Bernstein Institute of Physiology, Martin Luther University Halle-Wittenberg, Magdeburger Strasse 6, D-06097 Halle, Germany. Tel.: 49-345-557-1392; Fax: 49-345-557-4110; E-mail: wussling@med-phys.uni-halle.d400.de.

0006-3495/96/03/1144/10 $2.00

plasmatic calcium channels (e.g., smooth muscle) calcium waves in these cell types propagate much more slowly than in those with Ca^{2+}-sensitive endoplasmatic calcium channels (e.g., cardiac myocytes) (Rooney and Thomas, 1993; Williams, 1993; Sneyd et al., 1994). This fact points to the importance of the kinetics of the endoplasmatic calcium channels for the spreading of calcium waves (Rooney and Thomas, 1993). Surprisingly, calcium waves could also be observed in the SR-free single isolated cardiac myofibrils of a rabbit with a propagation velocity of only 15.5 μm/s at room temperature (Linke et al., 1993).

The propagation pattern of a calcium wave as revealed by a confocal laser scanning microscope (CLSM) is dependent on the location of the intracellular hot spot with respect to the confocal plane. This plane (or optical section) depicts a two-dimensional projection of a three-dimensionally expanding wave.The region within the confocal plane that is accessible to observation is relatively small because of the cell's diminutive size. To describe the shape and propagation pattern of calcium waves, extrapolations into the extracellular space were performed (Girard et al., 1992; Lipp and Niggli, 1993).

This study examines the proposition that the propagation velocity of the visible wave in a cardiac myocyte is expected to change with respect to time and distance of propagation and is only constant when the origin of the wave is localized in the confocal plane. The results do not conform to this hypothesis. We present a model to explain the unexpected results in terms of release, diffusion, and reuptake of activator calcium, and demonstrate that the propagation velocity essentially depends on the curvature of the calcium wave.

MATERIALS AND METHODS

Preparation and solutions

Rapidly excised hearts of adult Wistar rats were perfused in a Langendorff apparatus. The isolation of ventricular cardiomyocytes was carried out enzymatically and mechanically by stirring small tissue pieces according to standard procedure. Several filtered fractions of isolated cells were stored in buffered HEPES solution at room temperature. The composition of the solution was (mM): NaCl 110; KCl 2.6; $CaCl_2$ 1.8; $MgSO_4$ 1.2; KH_2PO_4 1.2; glucose 11; HEPES 25; albumin (Sigma) 1 mg/ml solution; penicillin/streptomycin (10,000 units/10 mg/ml; Biochrom) 0.1 ml/100 ml solution (pH 7.4 at 20°C). Freshly prepared cells were loaded with fluo-3 (Molecular Probes, Eugene, OR) by a 10-min exposure of 5 μM fluo-3 AM followed by a 30-min wash to remove the remaining extracellular calcium indicator. All experimental data presented were obtained at a temperature of 25°C.

Selection criteria

i) Myocytes with a diastolic sarcomere length of less than 1.8 μm were rejected. The mean sarcomere length (SL) was determined by image analysis with fast Fourier transform and amounted to 1.86 ± 0.05 μm (mean ± SD, n = 50). ii) Myocytes that did not shorten by at least 20% of the mean SL when electrically stimulated after a rest of 3 min were also omitted (ΔSL: 433 ± 48 nm, mean ± SD, n = 50). iii) From cells with spontaneously propagating calcium waves we selected those with a frequency of less than 1/min.

Perfusion chamber and CLSM

Part of the cell suspension was transferred to the 20-mm-diameter, 0.17-mm thick, glass bottom of a perfusion chamber. The suspension was covered by an identical second plate mounted in a perspex ring that was pressed against a rubber seal while screwing into the circularly shaped wall of the chamber. The solution layer was 0.5 mm in height and the chamber volume amounted to 200 μl. The chamber was mounted on the stage of an inverted microscope (Olympus IMT-2) belonging to the confocal laser scanning microscope INSIGHT PLUS (Meridian Instruments, Okemos, MI). The scan system consists of a galvanometer-driven bidirectional mirror (Brakenhoff), which allows image scanning of 512 times 480 pixels with a speed of 100 scans/s. The speed of image display amounts to 25 scans/s (CCD camera). The light source is an argon ion laser with emission wavelengths of 488 and 514 nm. The Z-drive accessory provides computerized control of optical sectioning, with a minimum vertical step of 0.6 μm. Image series showing calcium waves of rat heart cells stained with fluo-3 were saved on videotape.

Image processing

For the digitization of video frames we used a frame-grabber board with software package QuickCapture (Data Translation, Marlboro, MA) and a Macintosh IIci computer. The software used for both the calculation of intensity profiles and the presentation of images in this paper was IPLab Spectrum QC (Signal Analytics, Vienna, VA) and National Institutes of Health Image 1.43 (Microsoft). Fluorescence intensity profiles of propagating calcium waves were acquired from the very same region of interest (512 × 128 pixels), which was generally big enough to contain the whole optical section of the cell.

RESULTS

Fig. 1 shows the development of spherical calcium waves in two different cardiac myocytes. In the top of Fig. 1 we see a calcium wave starting at the upper edge of an oblong-shaped cell and expanding as a section of a circle, whereas the details of another oblong-shaped cell (*bottom*) show the development of the wave in the central part near the cell's end. To emphasize the latter wave pattern the contrast was strongly enhanced by "erosion." The rest between spontaneous calcium waves of both cells amounted to 2 min on average.

To determine wave speed, we selected those cardiomyocytes that exhibited spontaneously triggered calcium signals, starting at the very left or right end of the preparation. Fig. 2 (*top*) shows a typical example. The corresponding intensity profiles are shown in Fig. 2 (*bottom*). Note i) that the length calibration is different in each part of Fig. 2 and ii) the intensity profiles were determined from each "half" frame, as indicated in the bar on the right of Fig. 2 (*bottom*). For reasons of accuracy the position of the calcium wave was defined to be the point at which the increasing fluorescence of the running wave reached half-maximum.

In the following, we insert a theoretical consideration about the consequences of the two-dimensional depiction of a three-dimensional event. Fig. 3 (*top*) shows a scheme

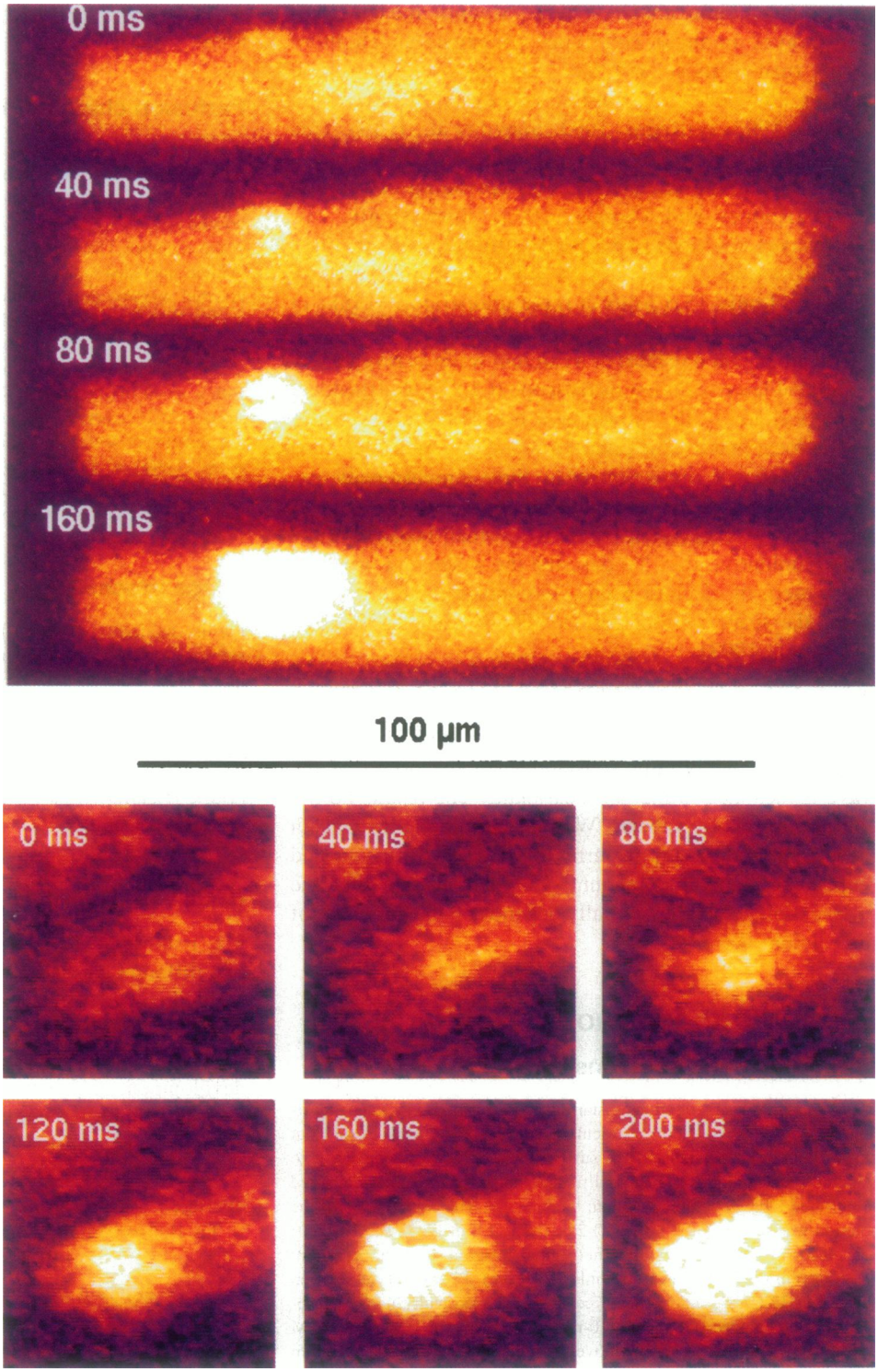

FIGURE 1 Two-dimensional depiction of the development of spontaneous spherical calcium waves revealed by confocal fluorescence microscopy from rat ventricular myocytes loaded with 5 μM fluo-3 AM. (*Top*) Expansion of a more hemispherical wave in an oblong-shaped cell. (*Bottom*) Details showing the development of a spherical calcium wave near the end of an oblong-shaped cardiac myocyte (noise reduced and excessively enhanced). Same length calibration in each part.

of several phases of an expanding spherical wave. Suppose that the origin F is localized in the confocal plane 0 and the propagation velocity is constant there, and the apparent wave speed measured, e.g., in confocal plane 2, is expected to change with respect to time and distance. In detail: If the velocity in confocal plane 0 is assumed to be constant then it may be expressed by $v = s/t$ (s = propagation length, t = time). A wave becomes visible in another confocal plane, but not until a certain delay given by z/v, where z means the distance of any confocal plane from plane 0. Therefore, the propagation time in any optical section is considered to be

$$t = \{\sqrt{(s^2 + z^2)}\}/v - z/v.$$

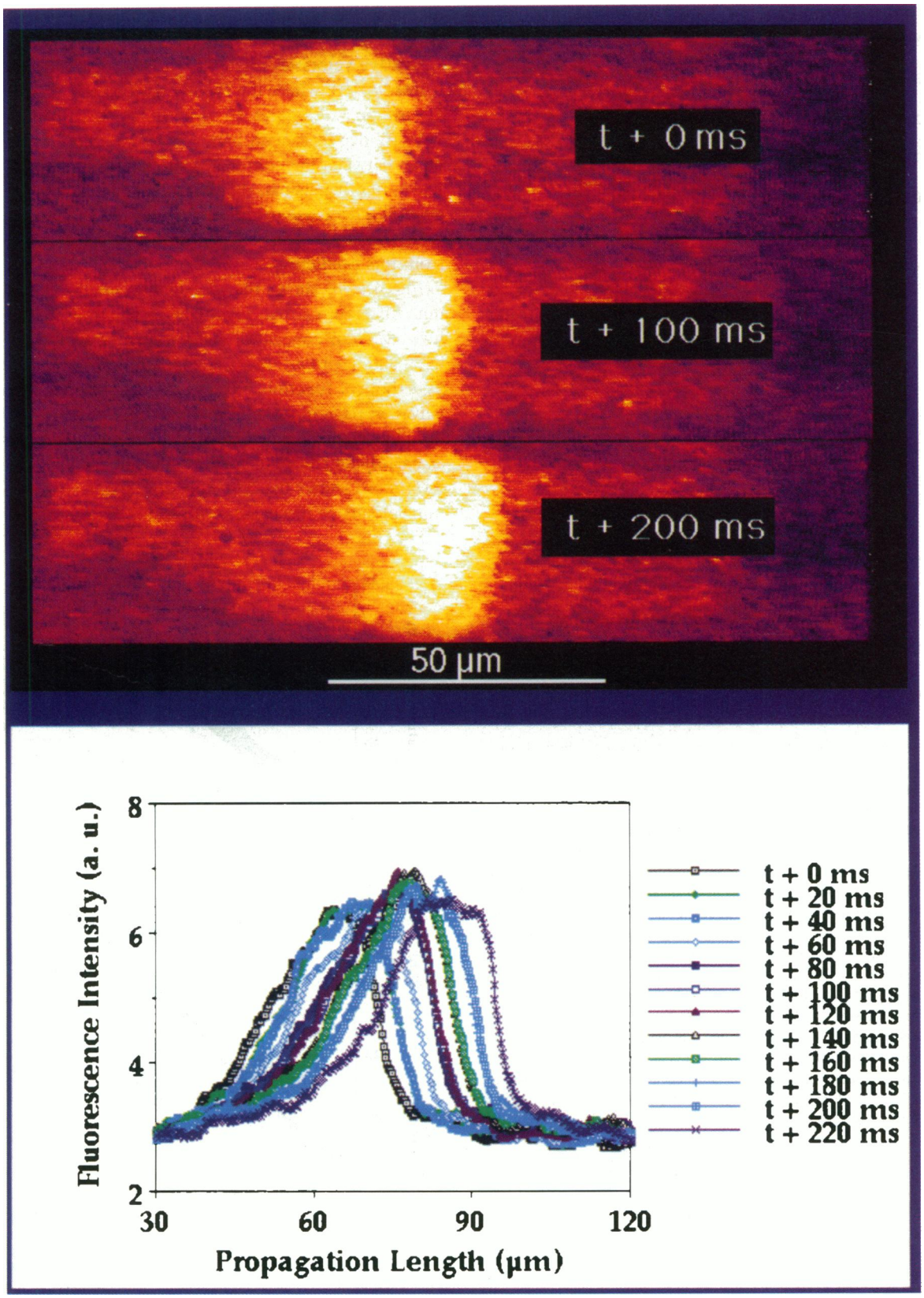

FIGURE 2 Propagation of a calcium wave at different moments. (*Top*) Cardiac myocyte loaded with 5 μM fluo-3 AM. (*Bottom*) Fluorescence intensity profiles acquired by imaging analysis at different moments and cell positions. Time-dependent position of calcium wave was set at that point where increasing intensity became half-maximum. Length calibration is different in each part.

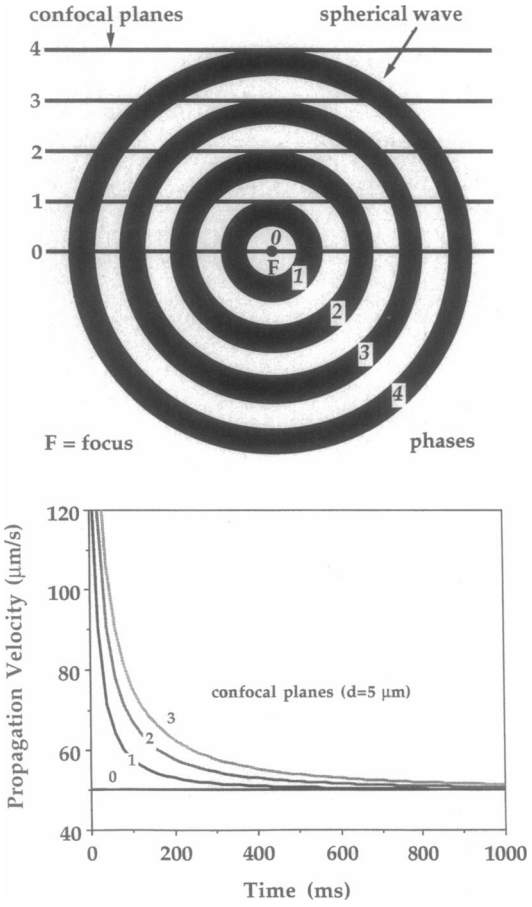

FIGURE 3 Schematical representation of an expanding spherical wave (*top*) and calculated propagation velocity versus time curves (*bottom*). (*Top*) A scheme shows the cross section of the wave at several phases in the z-direction of the confocal microscope. The wave is thought to originate from the focus F and to expand in all directions with constant velocity. Accordingly, the wave front reaches equidistant confocal planes, which are perpendicular to the z-direction after constant time intervals. Propagation velocity remains constant when determined in an optical section that is identical with that plane where the focus F is localized (see scheme, confocal plane 0). (*Bottom*) Propagation velocity versus time calculated for different confocal planes (indicated by numbers). A detailed explanation of how the curves were calculated is given in the text. Wave speed in plane 0 was set at 50 µm/s. Nonlinearity of wave speed with respect to time in optical sections outside of plane 0 is due to simple geometrical facts. Let $z = nd$ (n is the number of confocal plane, d is the distance of neighboring confocal planes, which was set at 5 µm). The curves ($ds/dt = f(t)$, Eq. 1) represent wave velocities related to the confocal planes with $z = 0$ µm ($n = 0$, where the focus F is located), 5 µm ($n = 1$), 10 µm ($n = 2$), and 15 µm ($n = 3$), respectively.

From this the corresponding propagation length

$$s = \sqrt{(v^2t^2 + 2vtz)}$$

is derived and the propagation velocity in a confocal plane is expected to obey the equation of the first derivative of s with respect to time:

$$ds/dt = (v^2t + vz)/\sqrt{(v^2t^2 + 2vtz)}. \quad (1)$$

Let n be the number of and d the distance between (neighboring) confocal planes, then $z = nd$. In Fig. 3 the amount of d was set at 5 µm and the wave speed in plane 0 at 50 µm/s. The curves of Fig. 3 ($\{ds/dt = f(t)\}$, *bottom*) represent wave velocities related to the confocal planes with $z = 0$ µm ($n = 0$, where the focus F is located), 5 µm ($n = 1$), 10 µm ($n = 2$), and 15 µm ($n = 3$), respectively. The velocity declines, with increasing time, the greater the distance between the confocal plane and the true origin of the wave. In other words, the scheme of Fig. 3 (*top*) predicts in general a decrease of the velocity of the calcium wavefront with respect to time. The following results are different from this prediction.

Fig. 4 (*top*) shows the propagation length versus time of nine different cardiac myocytes in solutions with extracellular calcium concentrations varying between 0.9 and 7.2 mM and (*bottom*) the corresponding means fitted by a hyperbolical function. We did not see a dependence of the wave propagation on the extracellular calcium concentration. Fig. 5 (*top*) shows the propagation velocity versus time as calculated from the data shown in Fig. 4 (*top*), and Fig. 5 (*bottom*) shows the corresponding means of the propagation velocity of these cells with respect to time. The velocity

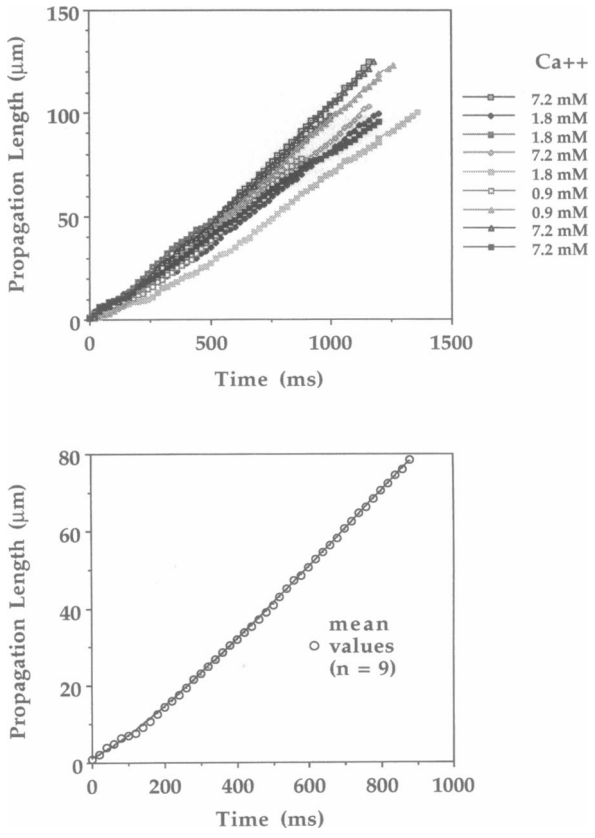

FIGURE 4 Dependence of the distance of wave propagation on time. (*Top*) Data of nine different ventricular rat cardiac cells. Calcium concentration of the perfusion solution was varied between 0.9 and 7.2 mM (see *right bar*). Temperature, 25°C. (*Bottom*) Approximation by the function $\{(s - p)/b\}^2 - \{(t - q)/a\}^2 = 1$, where s means distance of wave propagation and t stands for time. p, q are constants of the hyperbola. Circles are means of the data depicted at top. The curve approaches an asymptote, which is given by the slope $b/a = 0.112$ mm/s.

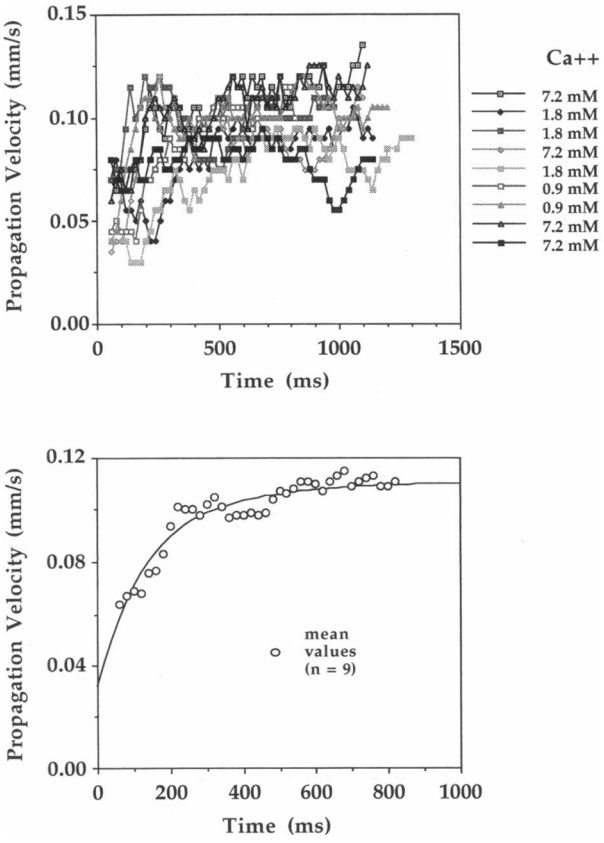

FIGURE 5 Dependence of the velocity of wave propagation on time as calculated from the data shown in Fig. 4. (*Top*) Different symbols of the velocity data represent various calcium concentrations of the perfusion solution (see *right bar*) and correspond to those of Fig. 4. (*Bottom*) Means of nine of these cells were approximated by the time derivative of the function used in Fig. 4: $ds/dt = (b/a)/\sqrt{\{(a^2/(t-q)^2 + 1\}}$. The maximum of the propagation velocity ds/dt is reached asymptotically (approximation results in $ds/dt_{max} = 0.112$ mm/s). The minimum of propagation velocity corresponds to the ordinate at $t = 0$ (extrapolation results in $ds/dt_{min} = 0.035$ mm/s).

data were approximated by a hyperbolic function with a calculated maximum velocity of 0.112 mm/s. Note that the velocity increases with time.

In detailed model simulations by several authors (Stern, 1992; Tang and Othmer, 1994; Sneyd and Kalachev, 1994; Bezprozvanny, 1994) we could not find direct implications of the nonlinearity of wave propagation. To better understand the experimental results presented here we wanted to simulate them simplistically.

If we assume that the amount of calcium released from the SR of any sarcomere is n_o at the time $t = 0$, then the time course of the concentration in the neighboring sarcomere is given by the equation

$$c(t) = (n_o/(4\pi Dt)^{3/2})\exp(-r^2/4Dt), \quad (2)$$

according to the conduction of heat in solids (Carslaw and Jaeger, 1959), D is the diffusion coefficient and r the diffusion path length. Actually, cytosolic calcium concentration is influenced by calcium sequestration and, therefore, the corrected time course of concentration is supposed to be

$$C(t) = c(t)\exp(-\alpha t), \quad (3)$$

where a is a simple constant. Fig. 6 (*top*) shows the decline of the calcium concentration with increasing distance from the locus of calcium release calculated at different times according to Eq. 3, with $D = 10^{-4}$ mm^2 s^{-1} and $a = 10$ s^{-1}. Fig. 6 (*bottom*) shows time courses of the concentration calculated at $r = 0.002$ mm (corresponding to a realistic sarcomere length). A threshold concentration must be exceeded to trigger the calcium release in the neighboring sarcomere. The time it takes to reach the threshold becomes shorter the more steeply the concentration increases. The parameter n, which stands for the amount of calcium released from the SR of a definite sarcomere, is dependent on

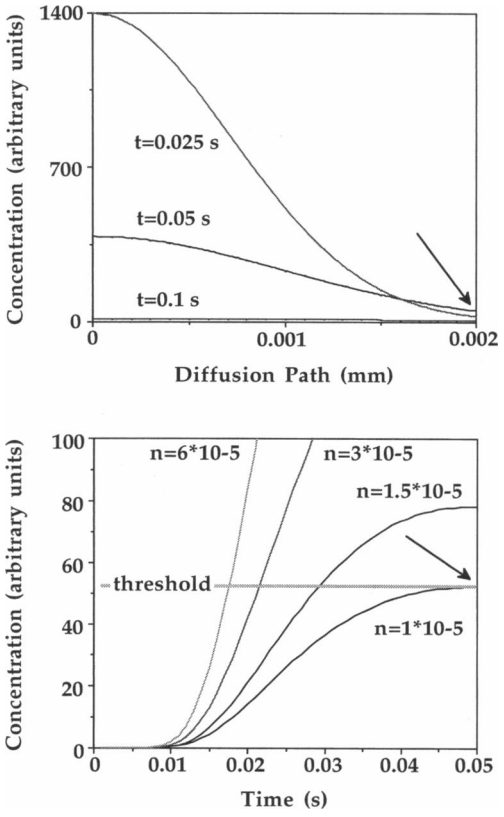

FIGURE 6 Calcium concentration profiles calculated according to Eq. 3, which is thought to reflect the diffusion of spontaneously released calcium from one sarcomere to the other (see text). The concentration is indicated in arbitrary units. (*Top*) Concentration versus diffusion path relationship at different moments as indicated by the numbers near the curves. A diffusion path of 0.002 mm is similar to the sarcomere length. The arrow points to the neighboring sarcomere with a local maximum of the concentration after about 0.05 s. (*Bottom*) Time courses of the concentration. Parameter n stands for the amount of calcium released from the SR in the preceding sarcomere and is indicated in arbitrary units. A threshold was set at that concentration which is reached after about 0.05 s with $n = 10^{-5}$ (see *arrow* pointing to the same value as in the upper part of that figure). Note that the steeper the concentration increase, the sooner the threshold is reached. For further explanation see text.

the preceding calcium release and is supposed to increase with distance while the wave is traveling from one sarcomere to the next. The arrows in Fig. 6 point to the threshold concentration that was reached in the first sarcomere after the start of the wave at $t = 0$ in the zeroth sarcomere.

To give an estimate of the diffusion coefficient from our experimental data, the dependence of wavefront velocity on curvature was determined. Fig. 7 (*top*) shows a plot of propagation velocity versus propagation length as obtained from the data shown in Figs. 4 (*bottom*) and 5 (*bottom*). The data (means, $n = 9$) was approximated by the relationship

$$N = c - K * D, \tag{4}$$

where N = normal propagation velocity of circular waves, c = propagation velocity of planar waves (c is expected to be about 0.112 mm/s according to Fig. 5), K = curvature (K is assumed to be 1/propagation length), and D denotes the diffusion coefficient. This relationship was used to further determine the critical radius R_{crit} for the outward propagation of waves in an excitable solution of the Belousov-Zhabotinski reaction (cf. Foerster et al., 1989) and predicts for $N = 0$

$$R_{crit} = D/c. \tag{5}$$

Below R_{crit} an outward propagation is expected to be impossible. If we plot the propagation velocity (N) versus 1/propagation length (curvature K, see Fig. 7, *bottom*) and apply Eqs. 4 and 5 to our data, an estimate of the diffusion coefficient $D = 3 * 10^{-4}$ mm^2/s and of the critical radius $R_{crit} = 2.7 \pm 1.4$ μm (mean ± SD) may be worked out.

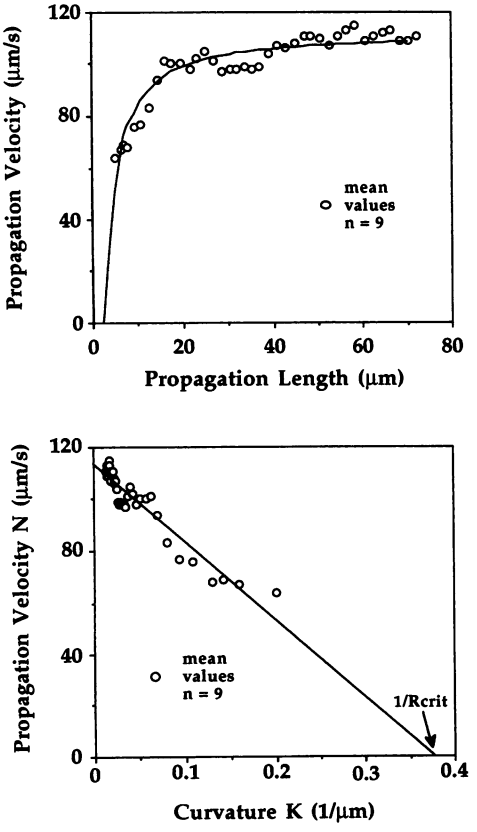

FIGURE 7 (*Top*) Propagation velocity versus propagation length of calcium wave. Circles are means ($n = 9$) and correspond to the data of both Fig. 4 (*bottom*) and Fig. 5 (*bottom*). Approximation of the velocity (N)-curvature (K) relationship $N = c - K^*D$ (Eq. 4; for explanation see text). (*Bottom*) Relation between curvature K and normal velocity N as determined from the data at the top. Approximation: $N = 113.2 - K^*0.302$, $r^2 = 0.9$. Velocity of planar wave $c = 113.2$ μm/s. For $N = 0$, $K = 0.37$. $1/K$ is the critical radius (Eq. 5) and results in $R_{crit} = 2.7 \pm 1.4$ μm (mean ± SD). Diffusion coefficient $D = c * R_{crit} = 3 * 10^{-4}$ mm^2/s.

DISCUSSION

Spontaneous contractile activity of isolated rat ventricular cardiocytes with a frequency of more than 1/min and a velocity of wavelike changes in fluorescence (fura-2) of approximately 100 μm/s was previously shown to be accompanied by a slight calcium overload (Wier et al., 1987). When considering only those cells that show spontaneous calcium waves (fluo-3) of less than 1/min and a rested state sarcomere shortening of 20% after field stimulation, we believe that the cytosolic calcium concentration of such cells (investigated in the present paper) is insignificantly enhanced and their functional properties are close to those of the group of quiescent cells with spatially homogeneous $[Ca^{2+}]_i$ (Wier et al., 1987).

The size of ventricular rat cardiocytes is not uniform and varies by 10 and 15 μm in the z-direction (Fabiato, 1981; 12.5 ± 3.3 μm according to our own unpublished confocal microscopic observations). From a simple geometrical consideration the presumption may be derived that the spherical calcium waves investigated in this paper would exhibit different propagation velocities in different confocal planes. This is explained above and summarized in Eq. 1, assuming that the wave velocity is constant in the confocal plane 0 (Fig. 3, *top*). In general, the wave speed in any optical section outside plane 0 is expected to decline with time as it travels from the focus through the cell. In the particular case where the plane of the focus of the wave is identical to the optical section that is chosen in the confocal laser scanning microscope, the real propagation velocity can be recorded.

As recently shown, calcium waves propagate faster in the longitudinal than in the transverse direction of rat cardiac myocytes (Engel et al., 1994), and wave velocity and calcium reuptake have been found to depend on temperature with different Q_{10} values (Engel et al., 1995). These data indicate that the spread of enhanced cytosolic calcium is due to both calcium diffusion after release from the SR and calcium sequestration. When related to constant experimental conditions the propagation velocity of spontaneous calcium waves was repeatedly reported to be constant (for a review see Williams, 1993).

The data presented in Figs. 5 and 7 clearly show that the propagation velocity increases in an unexpected manner with increasing time and increasing distance from the

wave's focus. In determining whether the phenomenon is genuine, two points are worth considering.

i) Fluorescence intensity profiles were determined from an area (region of interest including the whole cell) and not from a line (narrow area) within the cell. The determination of an intensity profile at the very beginning of a calcium wave is probably not completely correct if the wave appears as a half-circle, as implied in Fig. 1 (*top*). In this case the intensity profile, which is based on the measurement from an area, may be delayed in the initial phase. The wavefront in a rodlike cell, such as that shown in Fig. 2 (*top*), becomes practically planar after about 200 ms. The delay in question cannot account for the nonlinearity of the wave speed during the whole period of observation (see Fig. 5, *bottom*). The wave velocity was reported to be smaller in the transversal than in the longitudinal direction of the cell (Engel et al., 1994). A possible influence of anisotropic wave propagation on the determination of the longitudinal wave velocity is considered to be negligible in the initial phase of wave propagation and may be excluded completely when the transverse wave reaches the edge of the cell after a maximum propagation time of 200 ms (see figure 3 in Engel et al., 1994).

ii) Another relevant point is the influence of local sarcomere shortening on the position of the fluorescence intensity profile. Spontaneous contractile waves, as described previously (Kort et al., 1985; Golovina et al., 1986), follow calcium waves with a delay of 50–100 ms at room temperature (Wussling et al., 1994). Imagine that the calcium wave starts at one end of the cardiac myocyte and travels to the other. After less than 100 ms the contractile wave is starting run behind the calcium wave. The calcium wave is pulled back by the contractile wave to that end of the cell from which the wave originated, and this can result in an apparent diminution of the wave speed in the initial phase of both events. The regional cell shortening was shown to vary by 3 to 4 μm (Kort et al., 1985; Wussling, 1993), and because of this the velocity of the calcium wave might be reduced by 25% to 40% in the initial phase of propagation (up to 100 ms). A few tens of milliseconds later, the calcium and contractile waves are traveling with the same velocity. Therefore, this effect cannot account for the nonlinear increase of the calcium wave speed throughout the cell (see Fig. 5, *bottom*).

It may be suggested that the propagation velocity of a calcium wave is essentially dependent on its curvature. This was shown previously using an excitable solution of the Belousov-Zhabotinski reaction (Kuhnert et al., 1985; Foerster et al., 1989) and recently in oocytes of *Xenopus laevis* (Lechleiter and Clapham, 1992). According to the linear relationship between normal velocity and curvature of circular waves, the propagation velocity increases with decreasing curvature (i.e., with increasing propagation length). We are aware that the straight line shown in Fig. 7 (*bottom*) is fitted based on experimental data covering only 50% of the range of curvature. Therefore, the constants of the curvature velocity relationship, which were obtained by extrapolation, are considered to be estimated values. The negative slope of the straight line (Fig. 7, *bottom*) $-\mathrm{d}N/\mathrm{d}K$ resulted in an effective diffusion coefficient of $D = 3 * 10^{-4}$ mm^2/s, which corresponds well with those of cardiac myocytes reported by others (e.g., Tang and Othmer, 1994). As distinct from the effective diffusion coefficient, the free calcium diffusion coefficient, in the absence of calcium buffers, was taken to be slightly increased, i.e., 10^{-3} mm^2/s (Stern, 1992). The intersection with the velocity axis (Fig. 7, *bottom*) yields a value of $c = 113.2$ μm/s and agrees, of course, with the result of the approximation presented in Fig. 5, where a hyperbolic function was used to fit the data to reach the maximum wave velocity asymptotically. The normal wave velocity N becomes zero at curvature $K = 0.37$ (Fig. 7, *bottom*). The reciprocal value is supposed to represent the critical radius R_{crit} of the circular wave and was found to be 2.7 μm, below which an outward propagation will not take place. It has been shown that a spontaneous calcium spark could reflect the flux of calcium from a small number of cardiac RyRs acting in concert (Cheng et al., 1993). Both spontaneous and electrically evoked calcium sparks are limited to small cell volumes with a diameter of about 2 μm (FWHM) when the peak fluorescence level is reached (Cheng et al., 1995). The spark rate in rat ventricular myocytes is relatively low, and the CICR is not particularly sensitive to $[Ca^{2+}]_i$ under resting conditions in comparison to stimulated cells (Cannell et al., 1994). Thus, a number of sparks or a so-called macrospark, which can occur under resting conditions during calcium overload, is needed to initiate a propagating calcium wave (Cheng et al., 1993). If one accepts the estimated value of $R_{crit} = 2.7$ μm, the critical volume of a macrospark initiating a propagating calcium wave would amount to ~ 80 μm^3. Based on the data of Cheng et al. (1993, 1995) concerning the radius of a calcium spark (1 to 1.5 μm FWHM/2 at 10 ms), the critical volume mentioned is calculated to be occupied by at least six ($\{2.7$ μm/1.5 μm$\}^3$) and up to 20 ($\{2.7$ μm/1 μm$\}^3$) Ca^{2+} sparks. This means that the cytosolic calcium concentration above threshold must cover a region of at least two or (more likely) three sarcomeres across in the plane in which the focus is located. Otherwise we would not expect the initiation of a propagating calcium wave.

Once released from a sufficiently extended cluster of SR release channels calcium diffuses and will activate its neighbors. As depicted in Fig. 7 and discussed above, the propagation velocity is obviously dependent on the curvature of the wave. It may be suggested that at the initial phase of the calcium wave (i.e., at low radii), the volume into which released calcium diffuses is effectively increased. While traveling away the wave becomes more planar and the volume into which calcium diffuses becomes effectively smaller than at low radii. This leads to a steeper increase of the cytosolic calcium concentration after a certain diffusion path length (cf. Fig. 6, *bottom*). Thus the time taken to reach a critical threshold of $[Ca^{2+}]_i$ at the neighboring calcium release sites will decrease as the radius increases. This effect is the consequence of the summation of elementary events

(Ca^{2+} sparks), which was recently reported to cause nonuniformities in fluorescence during the early part of the electrically evoked $[Ca^{2+}]_i$ transient derived from the line scan "waterfall plot" (Cannell et al., 1994).

Based on model simulations a nonlinear relationship between propagation velocity and cytosolic calcium concentration was predicted (Stern, 1992). A proposed "spatially discrete model of calcium wave" assumes SR release sites located at the Z-lines. When cytosolic calcium exceeds the threshold, a fixed amount of calcium is released instantaneously at the Z-line and diffuses away. Free calcium is subject to instantaneous buffering and first-order uptake. The concentration at a point located a few sarcomeres away is found by solving the diffusion equation (with a linear uptake term) and summing the diffusion calcium fronts from all release sites. This results in an implicit relationship showing a nonlinear increase of propagation velocity with increasing local $[Ca^{2+}]_i$ (cf. equation 24 in Stern, 1992). An enhancement of $[Ca^{2+}]_i$ with increasing propagation length (or decreasing curvature of the wave) is most likely to be a consequence of the summation of elementary events (calcium sparks), as reported recently and mentioned above (Cannell et al., 1994). This effect would explain the nonlinear relationship of wave velocity versus propagation time or propagation length presented here (Figs. 5 and 7).

From Eq. 3 describing the time course of calcium concentration depending on diffusion path length and time (see Fig. 6), it may be easily derived that the propagation velocity of a calcium wave is also determined by the calcium pump activity of the SR, which is simulated by the term $\exp(-at)$. An impairment of the pump activity (simulated by the diminution of a) results in a steeper increase of the calcium concentration in the neighborhood of releasing sites. Thus the time to threshold decreases, and the wave velocity increases. Such an impairment of calcium pump activity probably occurs in dying cardiocytes, where wave velocities are markedly enhanced. We shall not fail to mention that even in SR-free cardiac myofibrils spontaneous calcium waves can travel from one end to the other, possibly because of periodic binding and unbinding of calcium ions to troponin (Linke et al., 1993). On the other hand, it could be demonstrated that after the application of the calcium chelator 1,2-bis(2-aminophenoxy)ethane-N,N,N',N'-tetraacetic acid to part of a rat ventricular myocyte a locally stimulated calcium transient did not propagate through the cell, although the SR was intact but not overloaded with calcium (Trafford et al., 1993).

In summary, an unexpected nonlinear increase of the propagation velocity of a spontaneous calcium wave is probably due to a local increase of the $[Ca^{2+}]_i$ with increasing radius of the wave while traveling along the cardiomyocyte. From the linear relationship of velocity versus curvature of the spherical wave a critical radius was worked out, below which an outward propagation will not take place. The experimental data appear to be inconsistent with the implications of a two-dimensional depiction of a three-dimensional spherical calcium wave in an optical section by confocal microscopy. We suspect that the expected decrease of the wave speed is covered by the supposed increase of cytosolic calcium at the expanding wave front.

We thank Dr. H. Opitz and Dr. Th. Mair for stimulating and helpful discussions, and S. Boldt and C. Girke for technical assistance.

This work was supported by the Deutsche Forschungsgemeinschaft.

REFERENCES

Allbritton, N. L., T. Meyer, and L. Stryer. 1992. Range of messenger action of calcium ion and inositol 1,4,5-trisphosphate. *Science.* 258: 1812–1815.

Berlin, J. R., M. B. Cannell, and W. J. Lederer. 1989. Cellular origins of the transient current in cardiac myocytes. *Circ. Res.* 65:115–126.

Bezprozvanny, I. 1994. Theoretical analysis of calcium wave propagation based on inositol (1,4,5)-triphosphate ($InsP_3$) receptor functional properties. *Cell Calcium.* 16:151–166.

Cannell, M. B., H. Cheng, and W. J. Lederer. 1994. Spatial nonuniformities in $[Ca^{2+}]_i$ during excitation-contraction coupling in cardiac myocytes. *Biophys. J.* 67:1942–1956.

Capogrossi, M. C., and E. G. Lakatta. 1985. Frequency modulation and synchronisation of spontaneous oscillation in cardiac cells. *Am. J. Physiol.* 248 (*Heart Circ. Physiol.* 17):H412–H418.

Carslaw, H. H., and G. C. Jaeger. 1959. Conduction of Heat in Solids, 2nd ed. Clarendon Press, Oxford.

Cheng, H., M. B. Cannell, and W. J. Lederer. 1995. $[Ca^{2+}]_i$ is inhomogeneous during the rising phase of the depolarization-evoked $[Ca^{2+}]_i$ transient. *Circ. Res.* 76:236–241.

Cheng, H., W. J. Lederer, and M. B. Cannell. 1993. Calcium sparks—elementary events underlying excitation-contraction coupling in heart muscle. *Science.* 262:740–744.

Engel, J., M. Fechner, A. J. Sowerby, S. A. E. Finch, and A. Stier. 1994. Anisotropic propagation of Ca^{2+} waves in isolated cardiomyocytes. *Biophys. J.* 66:1756–1762.

Engel, J., A. J. Sowerby, S. A. E. Finch, M. Fechner, and A. Stier. 1995. Temperature dependence of the mechanism of autocatalytic Ca^{2+} release in wave propagation. *Biophys. J.* 68:40–45.

Fabiato, A. 1981. Myoplasmic free calcium concentration reached during the twitch of an intact isolated cardiac cell and during calcium-induced release of calcium from the sarcoplasmic reticulum of a skinned cardiac cell from the adult rat or rabbit ventricle. *J. Gen. Physiol.* 78:457–497.

Foerster, P., S. C. Müller, and B. Hess. 1989. Critical size and curvature of wave formation in an excitable chemical medium. *Proc. Natl. Acad. Sci. USA.* 86:6831–6834.

Girard, S., A. Lückhoff, J. Lechleiter, J. Sneyd, and D. Clapham. 1992. Two-dimensional model of calcium waves reproduces the patterns observed in *Xenopus* oocytes. *Biophys. J.* 61:509–517.

Golovina, V. A., L. V. Rosenshtrauckh, B. S. Solev'ev, A. L. Undrovinas, and G. G. Chernaya. 1986. Wavelike spontaneous contractions of isolated cardiomyocytes. *Biophysics.* 31:283–289.

Ishide, N., T. Urayama, K. I. Inoue, T. Komaru, and T. Takishima. 1990. Propagation and collision characteristics of calcium waves in rat myocytes. *Am. J. Physiol.* 259 (*Heart Circ. Physiol.* 28):H940–H950.

Kort, A., M. Capogrossi, and E. Lakatta. 1985. Frequency, amplitude, and propagation velocity of spontaneous Ca^{++}-dependent contractile waves in intact adult rat cardiac muscle and isolated myocytes. *Circ. Res.* 57: 844–855.

Kuhnert, L., H.-J. Krug, and L. Pohlmann. 1985. Velocity of trigger waves and temperature dependence of autowave processes in the Belousov-Zhabotinsky reaction. *J. Phys. Chem.* 89:2022–2026.

Kushmerick, M. J., and R. J. Podolsky. 1969. Ionic mobility in muscle cells. *Science.* 166:1297–1298.

Lechleiter, J. D., and D. Clapham. 1992. Molecular mechanism of intracellular calcium excitability in *X. laevis* oocytes. *Cell.* 69:283–294.

Linke, W. A., M. L. Bartoo, and G. H. Pollack. 1993. Spontaneous sarcomeric oscillations at intermediate activation levels in single isolated cardiac myofibrils. *Circ. Res.* 73:724–734.

Lipp, P., and E. Niggli. 1993. Microscopic spiral waves reveal positive feedback in subcellular calcium signaling. *Biophys. J.* 65:2272–2276.

Niggli, E., and W. J. Lederer. 1990. Real-time confocal microscopy and calcium measurements in heart muscle cells: towards the development of a fluorescence microscope with high temporal and spatial resolution. *Cell Calcium.* 11:121–130.

O'Neill, S. C., J. G. Mill, and D. A. Eisner. 1990. Local activation of contraction in isolated rat ventricular myocytes. *Am. J. Physiol.* 258 (*Cell Physiol.* 27): C1165–C1168.

Rooney, T. A., and A. P. Thomas. 1993. Intracellular calcium waves generated by Ins(1,4,5)P_3-dependent mechanisms. *Cell Calcium.* 14: 674–690.

Sneyd, J., A. C. Charles, and M. J. Sanderson. 1994. A model for the propagation of intracellular calcium waves. *Am. J. Physiol.* 266 (*Cell Physiol.* 35):C293–C302.

Sneyd, J., and L. V. Kalachev. 1994. A profile analysis of propagating calcium waves. *Cell Calcium.* 15:289–296.

Stern, M. D. 1992. Theory of excitation-contraction coupling in cardiac muscle. *Biophys. J.* 63:497–517.

Stern, M. D., M. C. Capogrossi, and E. G. Lakatta. 1988. Spontaneous calcium release from the sarcoplasmic reticulum in myocardial cells. *Cell Calcium.* 9:247–256.

Tang, Y., and H. G. Othmer. 1994. A model of calcium dynamics in cardiac myocytes based on the kinetics of ryanodine-sensitive calcium channels. *Biophys. J.* 67:2223–2235.

Ter Keurs, H. E. D. J., P. H. Backx, P. P. De Tombe, and B. J. Mulder. 1988. Aftercontractions and excitation-contraction coupling in rat cardiac muscle. *Can. J. Physiol. Pharmacol.* 66:1239–1245.

Trafford, A. W., S. C. O'Neill, and D. A. Eisner. 1993. Factors affecting the propagation of locally activated systolic Ca transients in rat ventricular myocytes. *Pflügers Arch.* 425:181–183.

Wier, W. G., and L. A. Blatter. 1991. Ca^{2+}-oscillations and Ca^{2+}-waves in mammalian cardiac and vascular smooth muscle cells. *Cell Calcium.* 12:241–254.

Wier, W. G., M. B. Cannell, J. R. Berlin, E. Marban, and W. J. Lederer. 1987. Cellular and subcellular heterogeneity of $[Ca^{2+}]_i$ in single heart cells revealed by Fura-2. *Science.* 235:325–328.

Willams, D. A. 1993. Mechanism of calcium release and propagation in cardiac cells. Do studies with confocal microscopy add to our understanding? *Cell Calcium.* 14:724–735.

Williams, D. A., L. M. Delbridge, S. H. Cody, P. J. Harris, and T. O. Morgan. 1992. Spontaneous and propagated calcium release in isolated cardiac myocytes viewed by confocal microscopy. *Am. J. Physiol.* 262(*Cell Physiol.* 31):C731–C742.

Wussling, M. H. P. 1993. Sarcomere dynamics in small regions of cardiac cells measured by image analysis. *Biophys. J.* 64:220*a*. (Abstr.)

Wussling, M. H. P., R. Hüneke, and B. Husse. 1994. Sarcomere shortening and Ca^{2+}- transients in small regions of rat myocardial cells. *Eur. J. Physiol.* Suppl. 426, no. 6, R 80.